Available online at www.sciencedirect.com
SCIENCE DIRECT®
Journal of Power Sources 124 (2003) 124–132
JOURNAL OF POWER SOURCES
www.elsevier.com/locate/jpowsour

Chemical transformation of the electrode surface of lithium-ion battery after storing at high temperature

K. Araki, N. Sato*

Tochigi R&D Center, Honda R&D Co. Ltd., Tochigi 321-3393, Japan

Received 10 September 2002; received in revised form 14 January 2003; accepted 2 May 2003

Abstract

The deterioration behavior of the Li-ion batteries consisted of $LiMn_{1.7}Al_{0.3}O_4$ and hard carbon were investigated at the storage temperature from 50 to 75 °C. The deterioration phenomena were analyzed by using XPS, FT-IR, SEM and TEM for the negative electrode surface. As a result, the negative electrode surface of deteriorated battery showed the dissociation of manganese from the positive active material, and also the decomposition of electrolyte and $LiPF_6$ components was observed. When the storage temperature was over 65 °C, the ratio of PO_4^{3-} component in the films particularly increased, suggesting that the transformation was thought to be caused by the decomposition of $LiPF_6$. Furthermore, we developed the solid electrolyte interface (SEI) observation technology. The film thickness of the deteriorated negative electrode was found to be varied from 40 to 200 nm.

Keywords: Lithium-ion battery; Battery deterioration; Chemical transformation; Surface analysis; Solid electrolyte interface; TEM image

1. Introduction

After Li-ion batteries have been provided in the market since the beginning of 1990, the batteries have become a mainstream for cellular phone and notebook PC power supply with some advantages like small compact, lightweight and high energy. Further, Li-ion batteries are expected as a power supply for hybrid electric vehicle (hereinafter, HEV) with lightweight and high power performances.

However, batteries for HEV use are exposed to severer temperature environment than those for public commercial product like cellular phones. Accordingly, durability against high temperature should be attained for HEV application. It is known that a battery deterioration takes place during both cycling and storage, even if Li-ion batteries are used or stored at room temperature. This tendency will be more remarkable at high temperature over 40 °C.

In this way, cycle life and calendar life of Li-ion batteries at high temperature are big issues for HEV application. Several papers were reported regarding the deterioration mechanism of Li-ion batteries with storage condition at high temperature environment. Norin et al. [1], for example, reported the increase of dc impedance due to a swelling of separators in Li-ion batteries.

In addition, Sloop et al. [2] reported that the durability of $LiPF_6$ as an electrolyte salt of Li-ion batteries against high temperature was not enough. In this paper, Li-ion batteries stored at high temperature environment over 50 °C were dismantled under N_2 gas atmosphere, and the deterioration mechanisms with several storage conditions were studied by analyzing the generated films on the negative electrode with XPS, FT-IR, SEM and TEM images.

2. Experimental

2.1. Calendar life at high temperature

The high power Li-ion batteries consisted of hard carbon as negative active material, 1 M $LiPF_6$ ethylenecarbonate (EC), diethylcarbonate (DEC) and dimethylcarbonate (DMC) as electrolyte, and $LiMn_{1.7}Al_{0.3}O_4$ as positive active material. Calendar life test was performed at high temperature between 50 and 75 °C shown in Table 1. A reversible capacity, dc impedance, and ac impedance of each battery were measured every 13 days. The reversible capacity was defined as discharged capacity with (1/3)*C* at 25 °C.

Test profile of a pulse power characterization with SOC 100 and 50% was shown in Fig. 1. The dc impedance

* Corresponding author. Tel.: +81-28-677-6790; fax: +81-28-677-6786.
E-mail addresses: kazuhiro_araki@n.t.rd.honda.co.jp (K. Araki), noboru_sato@n.t.rd.honda.co.jp (N. Sato).

0378-7753/$ – see front matter © 2003 Elsevier B.V. All rights reserved.
doi:10.1016/S0378-7753(03)00593-7

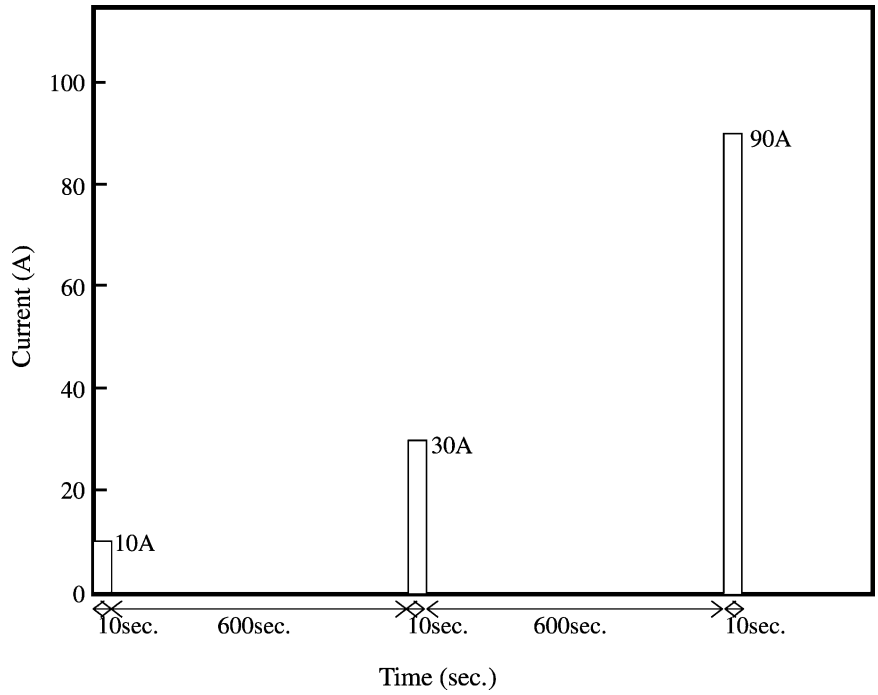

Fig. 1. Applied pulse profile for dc impedance.

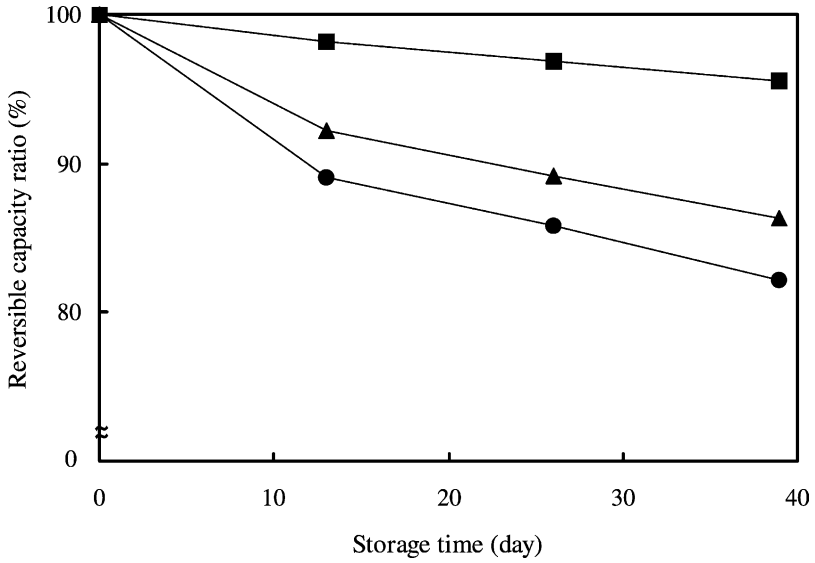

Fig. 2. The change of reversible capacity with various storage time: (■) 50 °C; (▲) 65 °C; (●) 75 °C.

was calculated from the gradient between the current and voltage data at 10 s. discharge. On the other hand, the ac impedance was measured by the constant current control of 500 mA at the frequency from 10 mHz to 20 kHz.

Table 1
Test conditions for calendar life

Storage temperature (°C)	50	65	75
Storage SOC (%)		75	
Storage time (days)		39	

2.2. Quantitative analysis of phosphorous in electrolyte

Electrolyte from the stored batteries was diluted with 5 ml ethanol in a glove box under N_2 gas atmosphere. The electrolyte sample of 0.15 g was then diluted with nitric acid. Phosphorus was measured by means of ICP emission spectrophotometer of SEIKO Instruments Inc. (SPS4000).

2.3. Analysis by FT-IR

Negative electrode samples from the stored batteries were analyzed by ATR-FT-IR with the incident angles of 30,

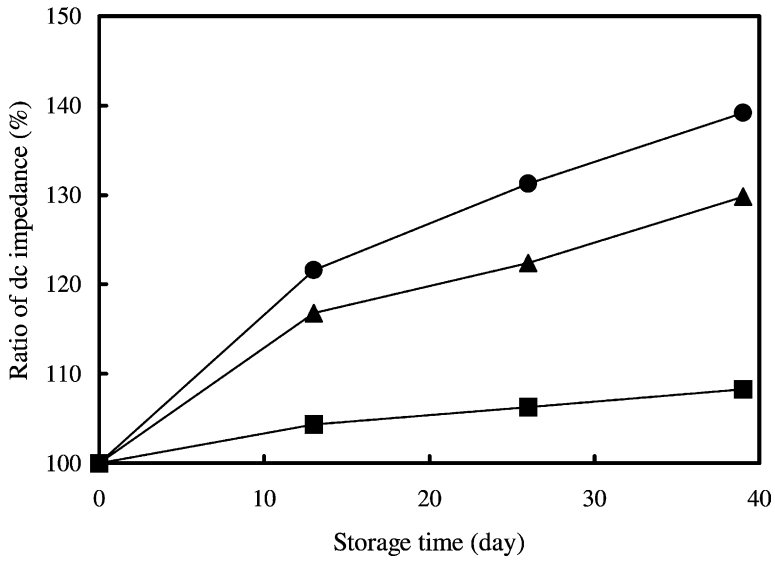

Fig. 3. The change of dc impedance with various storage time: (■) 50 °C; (▲) 65 °C; (●) 75 °C.

40, 50, 60° using FTS-55A spectroscope (BioRad Digilab). Samples were transferred and measured under N_2 gas atmosphere.

2.4. Analysis by XPS

The batteries were dismantled in the glove box and small pieces of negative electrode were mounted without being washed by any solvent on XPS sample holders. These samples were transferred to the XPS chamber under N_2 gas atmosphere without exposure to air. XPS measurement was conducted by SSX-100 (SSI) using a monocrystal spectral Al Kα ray as X-ray source. The etching of samples for depth profile analysis was carried out with Ar ion laser (3 keV SiO_2 conversion with 6.4 nm/min).

2.5. Surface morphology observation of negative electrode

2.5.1. Analysis by SEM

The batteries were dismantled in the glove box under N_2 gas atmosphere as pre-conditioning. The small sample was collected from the negative electrode and introduced to SEM chamber under the N_2 gas atmosphere. The equipment was S-5000 (Hitachi) with the accelerating voltage of 6 keV.

2.5.2. Analysis by TEM

The thin film sample of negative electrode was made with focused ion beam (FIB). TEM image was observed using analytical electron microscope HF-2210 (Hitachi) with field emission type.

3. Results and discussion

Figs. 2–4 show the changes of reversible capacity, the dc impedance and the ac impedance with various storage con-

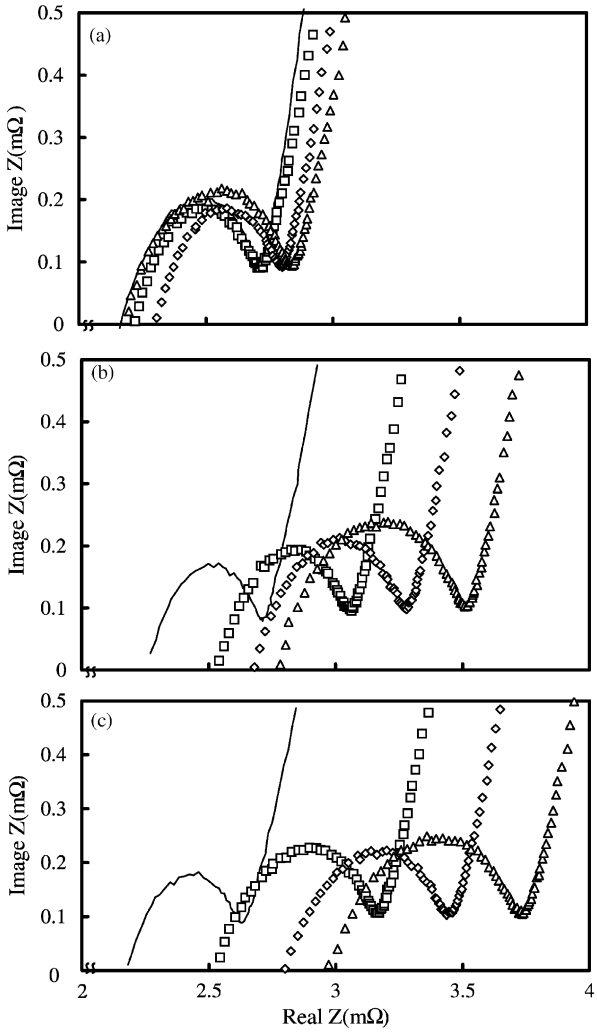

Fig. 4. Impedance profiles with various temperature at SOC 50% at (a) 50 °C, (b) 65 °C and (c) 75 °C: (—) 0 day; (□) 13 days; (◇) 26 days; (△) 39 days.

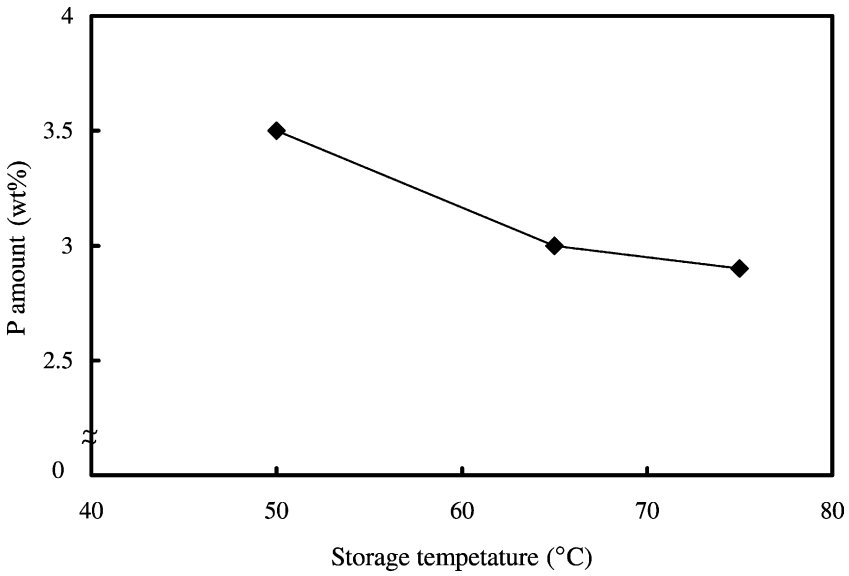

Fig. 5. The relationship between storage temperature and phosphorous amount in the electrolyte.

ditions, respectively. The ac impedance contains a solution resistance and a charge transfer resistance. We confirmed the big difference between the deterioration velocity at 50 °C storage and that at 65 °C storage or higher.

Fig. 5 shows that the relationship between storage temperature and phosphorous amount in the electrolyte. The phosphorous amount decreased in accordance with the increase of storage temperature, and especially at 65 °C. The fact implies that the decomposition of $LiPF_6$ was accelerated at 65 °C or higher and then the decreasing of phosphorous amount took place.

It is known that the solid electrolyte interface (SEI) films are formed on negative electrode in the first charge that corresponds to activation process [3]. And it was reported that the SEI would be necessary to intercalate and de-intercalate Li^+. Here, we analyzed the negative electrode surface to reveal the components of SEI by using FT-IR and XPS.

In the FT-IR analysis shown in Fig. 6, the peaks that attributed to lithium alkyl carbonate (LiOCOOR) were observed on all the samples. Furthermore, the absorption peaks attributed to carboxylic acid in 1600–1550 cm^{-1} and those attributed to phosphoric acid in 1100–900 cm^{-1} increased

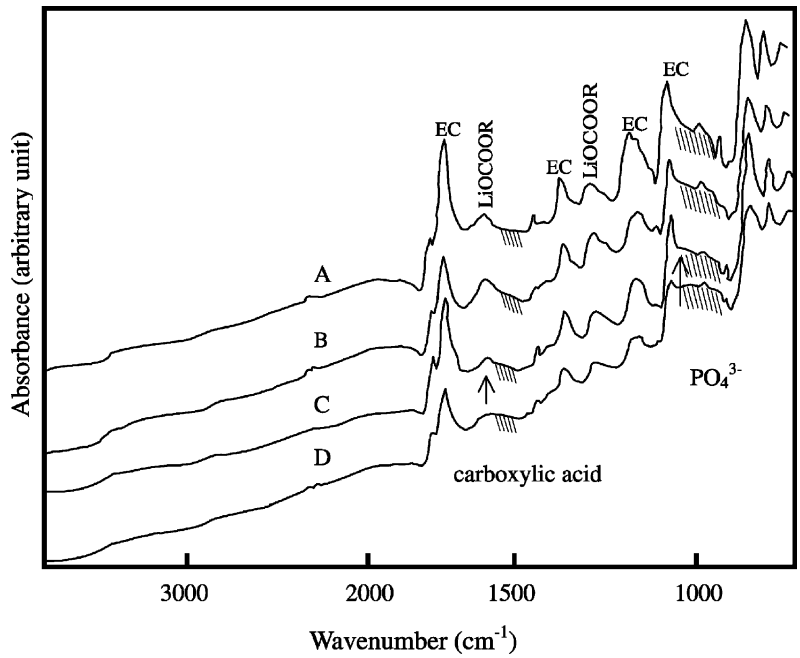

Fig. 6. FT-IR spectra for the negative electrode surface at various temperature: (a) without storage; (b) 50 °C; (c) 65 °C; (d) 75 °C.

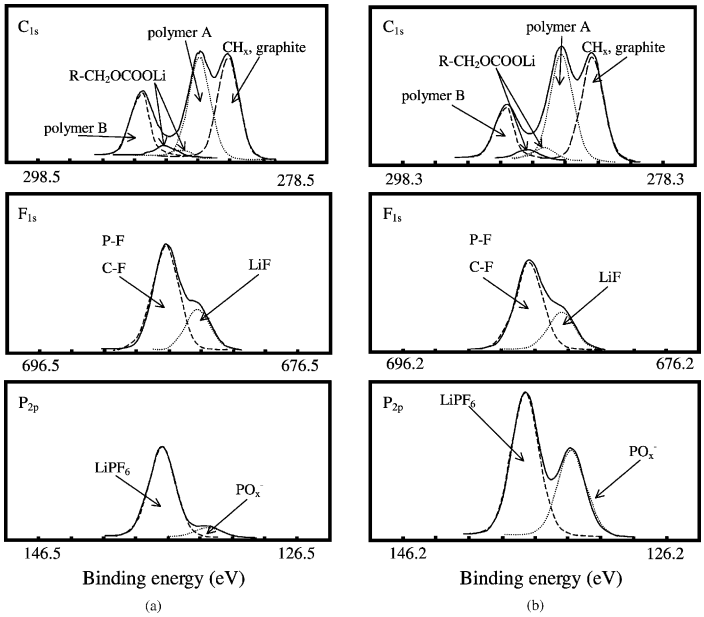

Fig. 7. XPS spectra for the negative electrode without storage (a) and with storage (b) at 65 °C.

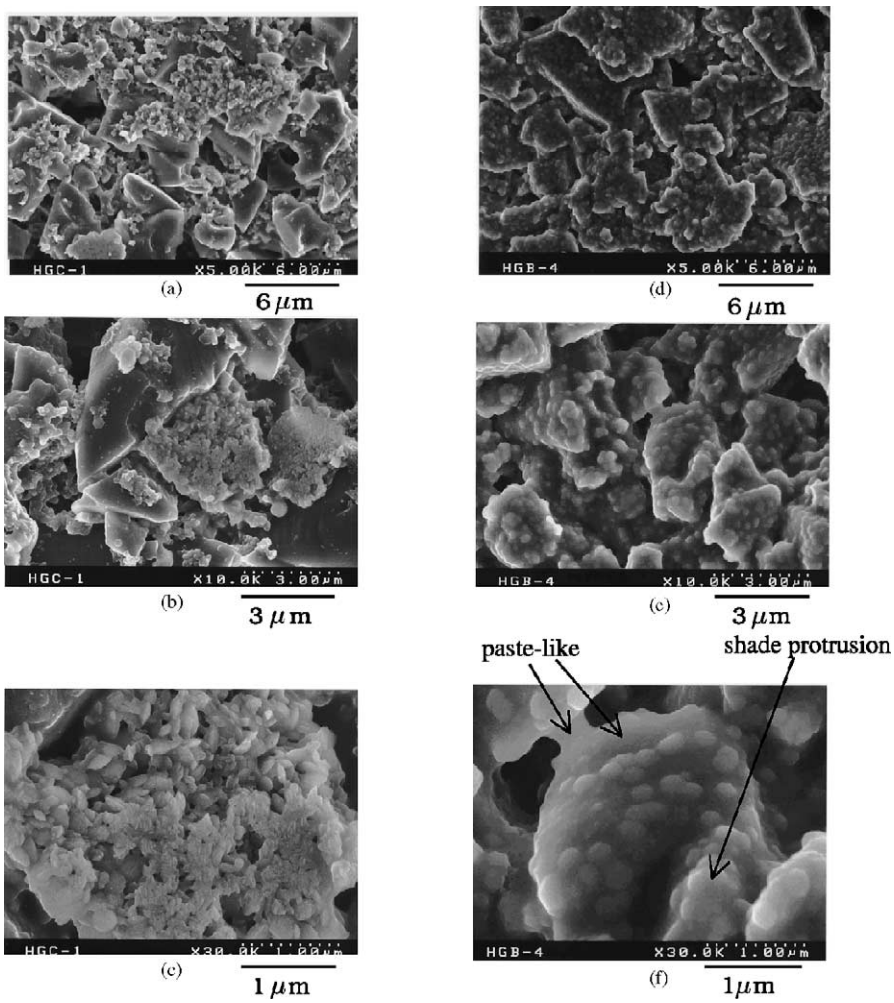

Fig. 8. SEM micrographs of the negative electrode surface: (a–c) without storage; (d–f) storage at 65 °C.

in accordance with the storage temperature rise. When we compared C_{1s} spectra for the unstored and stored samples from XPS results shown in Fig. 7, the ratio of the organic components was almost equivalent between these samples. The peaks of $LiPF_6$ is attributed to the electrolyte salt precipitated in the surface of the samples, since the samples for XPS measurement were not washed.

The organic components in films were consisted of polymer A and polymer B. The peak at 285.5–286.5 eV corresponded to polymer A containing R–$CH_2OCOOLi$, and the other peak at 290 eV corresponded to polymer B. It is thought that the polymer A was formed by ring-opening product from EC and DMC [4]. The polymer A will be expressed as [–CH_3($OOCOCH_2CH_2OCOO$)–CH_3–] [2,5]. On the other hand, the polymer B was formed by the reactions (1) and (2) as the polymerization of EC [3]:

$$EC \rightarrow [(CH_2CH_2O)_mCOO]_n + CO_2 \quad (1)$$

$$EC \rightarrow LiOCOOCH_2CH_2OCOOLi \quad (2)$$

SEM images of negative electrode were indicated in Fig. 8. No deposited film was observed on the unstored sample, but the deposited films were confirmed on the stored sample. The observed area of XPS is ellipse with 1000 μm × 1750 μm which is much wider area than that of SEM. Accordingly, it is not able to distinguish the difference of local film presence from the analyzed data by XPS and FT-IR.

The morphology of stored film showed the quite difference from that of unstored one. Fig. 8 showed that the stored film was consisted of the shade protrusions and the paste-like element. Accordingly, any new surface deterioration took place in the stored film by the action of stored condition.

The cross-sectional observation of negative electrode stored at 65 °C by TEM was carried out to recognize the SEI and to measure the thickness of SEI. The observed images were shown in Fig. 9.

The dark area corresponded to the carbon negative electrode and the light area referred to SEI. The film thickness of the sample was varied from 40 to 200 nm. The film area was almost homogeneous but there were some points which contain particulate substances as observed in Fig. 9(b). Most of the films observed by TEM image refer to the light contrast in Fig. 9(b). And also, it was thought that those films corresponded to the paste-like component which was observed by SEM image shown in Fig. 8(f). As a result, the

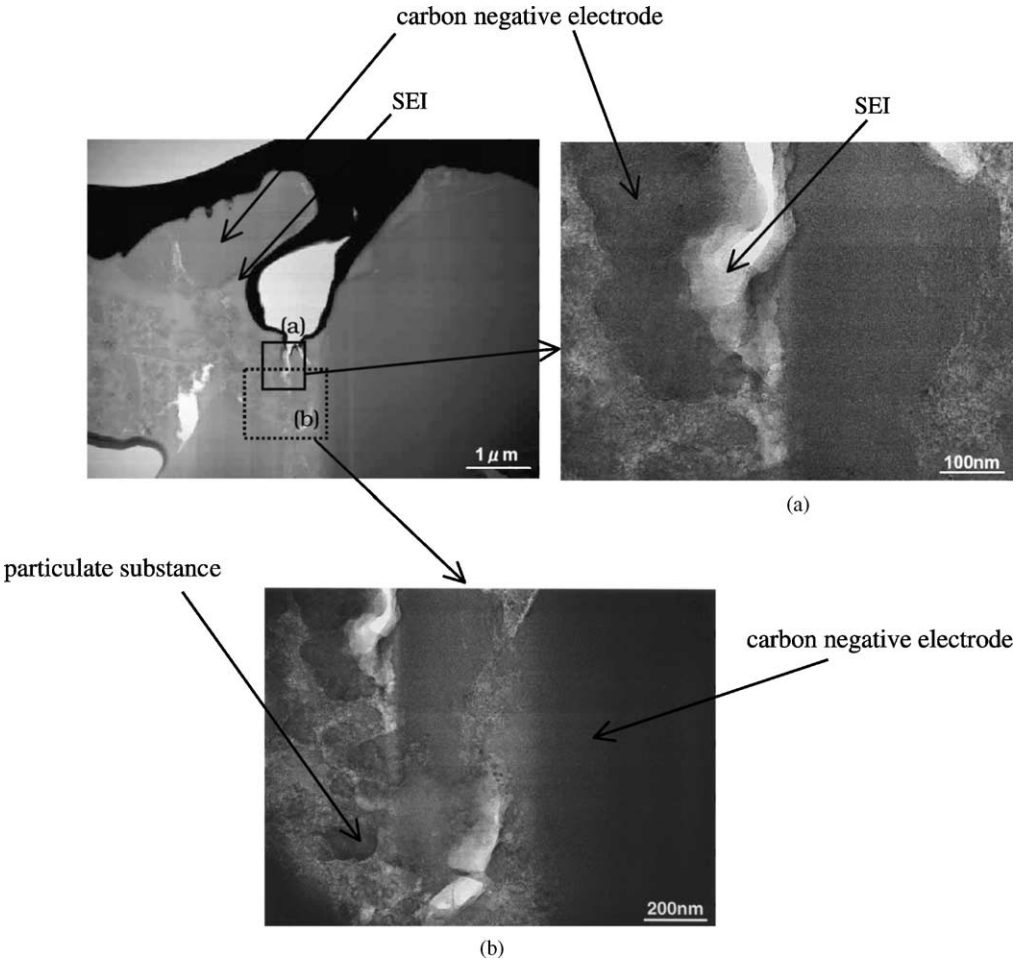

Fig. 9. TEM micrographs of the negative electrode surface stored at 65 °C.

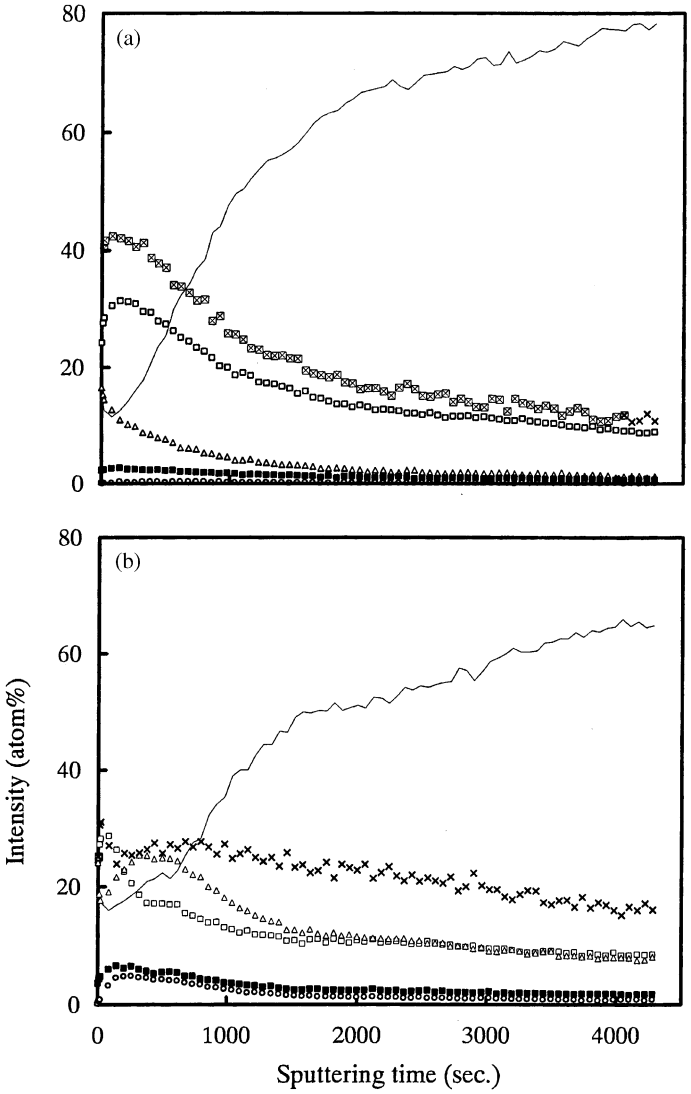

Fig. 10. Depth profiles of each element in the SEI without storage (a) and with storage at 75 °C (b): (—) C_{1s}; (□) F_{1s}; (△) O_{1s}; (×) Li_{1s}; (■) P_{2p}; (○) Mn_{2p^3}.

increase of film thickness will cause the deterioration of batteries.

We investigated the film component from results of XPS depth profile shown in Fig. 10. We confirmed that the peak intensity for Li_{1s} coincided with that for F_{1s} in Fig. 10(a). Further, the peak intensity for Li_{1s} coincided with that for O_{1s} and the peak intensity for P_{2p} coincided with that for Mn_{2p^3} in Fig. 10(b).

Fig. 11 refers to the distribution of each component in the surface layer on the negative electrode. There are some differences between the unstored electrode and the stored one. Major difference was observed on the peak intensity of P_{2p} and Mn_{2p^3} in accordance with the sputtering.

As Fig. 11 showed that the peak intensity of P_{2p} corresponded to PO_x^- and $LiPF_6$, it was found that LiF and PO_4^{3-} derived from the decomposition of $LiPF_6$ were detected over the whole depth of SEI.

The decomposition reactions of $LiPF_6$ will be expressed as the reactions (3) and (4) [3,4]. The detected Mn in the stored sample thought to be dissociated from the positive active material of spinel manganese which was attacked by HF according to the reaction (5):

$$LiPF_6 \rightarrow LiF \downarrow + PF_5 \uparrow \quad (3)$$

$$PF_5 + H_2O \rightarrow 2HF + POF_3 \quad (4)$$

$$2LiMn_2O_4 + 4H^+ \rightarrow 3\lambda\text{-}MnO_2 + Mn^{2+} + 2Li^+ + 2H_2O \quad (5)$$

These reactions will be revitalized by the action of high temperature storage. Though Li^+ and Mn^{2+} will transfer to the surface of carbon negative electrode by the charge process during the measurement of battery capacity every 13 days, only Li^+ intercalated into the carbon layers.

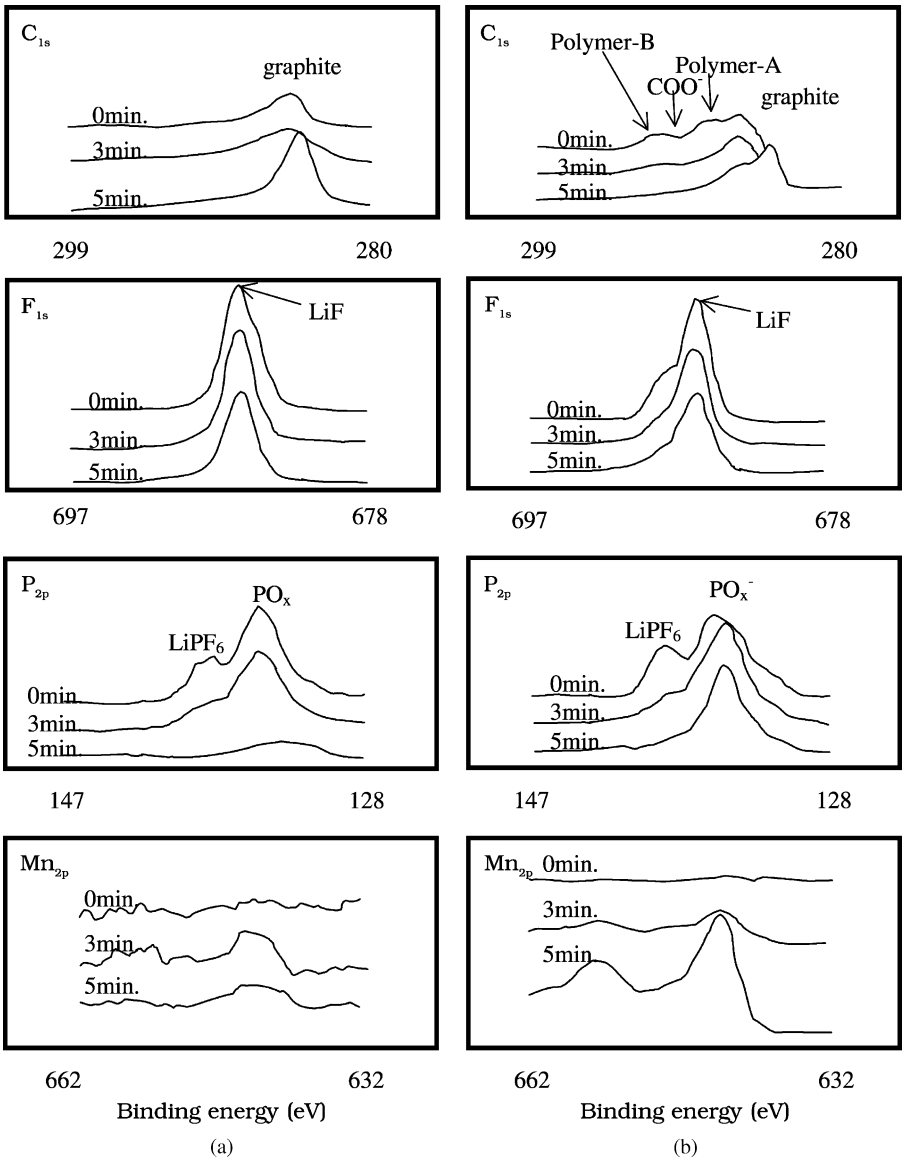

Fig. 11. XPS spectra for the negative electrode without storage (a) and with storage (b) at 65 °C in accordance with the sputtering time.

The ionic radius of Mn^{2+} with 0.083 nm is almost same as Li^+ with 0.076 nm [6]. However, Mn^{2+} is never intercalated like Li^+. Kumagai et al. [7] reported that the redox potential of Mn/Mn^{2+} in electrolyte was estimated as 1.79 V versus Li/Li^+ and this reason caused the reduction of Mn^{2+} by the contact with the negative electrode. It implies that Mn^{2+} would deposit as Mn metal or MnO_2 on the negative electrode. The observed data of Fig. 11

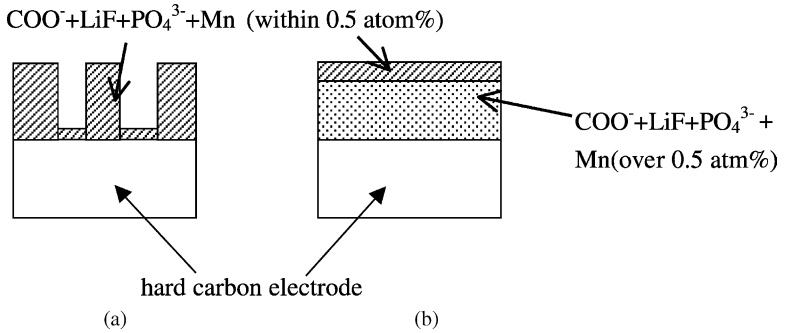

Fig. 12. Simplified schematic model for the surface compounds of negative electrode without storage (a) and with storage at 65 °C (b).

supported the Mn deposition by the action at high stored temperature.

Fig. 12 shows the proposed model diagrams of component distribution for the surface of the unstored and stored negative electrodes based upon Fig. 11. The formed COO^- in Fig. 11 will be attributed to the polymerized EC and lithium alkyl carbonate considering XPS results.

Kwon and Evans [8] reported that the viscosity of electrolyte increased by the contact with carbon electrode. We thought that the viscosity of electrolyte would increase the polymerization of EC. The lack of electrolyte components will cause the diffusion delay during the discharge process. Therefore, Li^+ has still left in SEI and then the oxygen from the polymerized EC in SEI will be supplied to form Li_2O.

4. Conclusion

(1) We confirmed the difference between film thickness of negative electrode surface for the unstored battery and that for the stored battery. The degradation of battery will be caused by the film generation.
(2) The thickness of SEI on the stored negative electrode was not uniform and it was varied from 40 to 200 nm.
(3) The films were formed by the decomposed products from $LiPF_6$, polymerized EC, and Mn dissociated from the positive active material.
(4) Three directions to improve the deterioration of negative electrode for calendar life of the batteries are as follows: (i) durability improvement of $LiPF_6$ against high temperature, (ii) polymerizing depression of EC and (iii) inhibition of Mn dissociation from spinel Mn as positive active material.

References

[1] L. Norin, R. Kostecki, F. McLarnon, Electrochem. Solid-State Lett. 5 (2002) A67.
[2] S.E. Sloop, J.K. Pugh, S. Wang, J.B. Kerr, K. Kinoshita, Electrochem. Solid-State Lett. 4 (2001) A42.
[3] Y. Ein-Eli, Electrochem. Solid-State Lett. 2 (1999) 212.
[4] A.M. Anderson, K. Edström, J. Electrochem. Soc. 148 (2001) A1100.
[5] K. Edström, M. Herranen, J. Electrochem. Soc. 147 (2000) 3628.
[6] Shannon, Acta Cryst. A32 (1976) 751.
[7] N. Kumagai, S. Komaba, Y. Kataoka, M. Koyanagi, Chem. Lett. 2000 (2000) 1154.
[8] K. Kwon, J.W. Evans, Electrochem. Solid-State Lett. 5 (2002) A59.